Anatoliy Vorobev[1,*]
Artem Antonov[2]
Galina Nazarova[2]
Elena Ivashkina[2]
Emiliya Ivanchina[2]
Vyacheslav Chuzlov[2]
Toleubek Kaliyev[2,3]

Development of a Two-Fluid Hydrodynamic Model for a Riser Reactor

ANSYS Fluent is used to examine the mixing of catalyst zeolite particles with petroleum feedstock and water vapor in a fluid catalytic cracking (FCC) riser. A two-fluid model is developed for tracking catalyst particles and gas mixture in a riser, modeling the granular and gaseous phases as two interpenetrating continua. The hydrodynamic flows are analyzed with the aim to single out the principal physical effects that determine the distribution of particles. The results are compared with a study that is based on a non-isothermal reactive model. It is demonstrated that the simplistic purely hydrodynamic model generates similar flow fields. The developed model is valuable for improvements of modern FCC risers. The model is applied for understanding the hydrodynamics of an S-200 KT-1/1 industrial unit.

Keywords: Catalytic cracking, Hydrodynamic modeling, Multiphase flow, Two-fluid model

Received: November 24, 2021; *revised:* January 26, 2022; *accepted:* February 04, 2022

DOI: 10.1002/ceat.202100596

Supporting Information available online

1 Introduction

Catalytic cracking is the most common industrial process to break down the long-chain vacuum gasoil hydrocarbons into lighter and more commercially useful products such as gasoline, diesel, and light olefins, i.e., ethylene and propylene, in particular, that are needed in very large quantities mainly for production of plastics. In oil and gas industry, numerical modeling is widely employed for development of novel, improved technologies. Incorporation of computational fluid dynamics (CFD) solvers for detailed understanding of the hydrodynamic (mixing) aspects of the flow chemical reactors is a common element of all recent numerical models [1].

Modeling of a reactive fluid flow in a fluid catalytic cracking (FCC) riser is complicated by an enormous number of chemical transformations that may happen in the process. For computationally less expensive modeling, reaction schemes are simplified by grouping the chemicals into lumps. Selection of a reaction scheme frequently predefines the physical effects that can be captured by the model. For instance, the first kinetic model was proposed by Wickman and Nays [2], who introduced three lumps: feedstock, gasoline, and all other components which include various light gases and coke. Since, in this model, coke and light gases are represented as a single lump, description of heat/mass transfer between gaseous and solid phases, including coke deposition on catalyst, is not possible. A more sophisticated ten-lump kinetic model which includes a "dry gas" component was introduced by Jacob et al. [3]. In their work, in addition to coking, the authors describe other undesirable thermal cracking reactions that occur in a high-temperature section of a riser. Understanding of kinetics and thermodynamics of the industrial FCC process is also the focus of our recent works [4–8].

Gan et al. [9] developed an eleven-lump model, with the aim to further enhance the performance of FCC risers for greater propylene yields to meet demands of a fast-growing propylene market. Young et al. [10] incorporated this kinetic scheme into a comprehensive hydrodynamic model which they developed on the basis of the ANSYS Fluent software.

In addition to complex chemistry, modeling of processes in an FCC riser is complicated by complex hydrodynamics of a heterogeneous mixture of gases, liquids, and solids. Modeling of a three-phase three-dimensional flow with the account of heat transfer, evaporation of droplets, and chemical reactions was carried out in [11], which adopts a continuous Eulerian approach for description of phases. In [12], the authors used a similar approach with the aim to optimize the feedstock injection. They found that intensive mixing of chemical components accelerates the mass transfer and increases the yield of desired products. On the other hand, it is also recommended to avoid the prolonged contact between catalyst and feedstock as this helps to keep the desired products from further (unwanted) cracking and coking reactions. In particular, it is

[1]Dr. Anatoliy Vorobev
A.Vorobev@soton.ac.uk
University of Southampton, Faculty of Engineering and Physical Sciences, University Road, SO17 1BJ Southampton, UK.

[2]Artem Antonov, Dr. Galina Nazarova, Prof. Elena Ivashkina, Dr. Emiliya Ivanchina, Dr. Vyacheslav Chuzlov, Toleubek Kaliyev
National Research Tomsk Polytechnic University, Division for Chemical Engineering, 30 Lenin Avenue, Tomsk, 634050, Russia.

[3]Toleubek Kaliyev
PLC "Pavlodar Petrochemical Plant", 1 Khimkombinatovskaya Street, 140000, Pavlodar, Republic of Kazakhstan.

found that the optimal angle for the feedstock injection pipes to produce the flow in a reactor with the most desirable characteristics is 30°.

There are a few other studies that investigated the hydrodynamic flows in an FCC riser. In particular, Huang et al. [13] measured the particle velocity and solid particle retention by an experimental study using fiber optic probes. Idris and Berne [14] used the ANSYS CFX software to create a lump-free kinetic model. Their geometries, however, remain quite different from real FCC risers with the height and width of the modeled column equal to 15.1 m and 0.1 m, which was approximately half and about 10 % of the actual riser's height and width.

The focus of the current work is the hydrodynamic modeling of the process of catalytic cracking, movement of catalytic particles, and mixing of particles with feedstock and water vapor. In this work, a macroscopic two-fluid Eulerian-Eulerian model is developed for tracking the evolution of zeolite catalyst and petroleum feedstock. Specifically, the mass and heat transfer processes are simulated in an FCC riser from the S-200 KT-1/1 industrial unit.

2 Physical and Mathematical Models

Modeling of the hydrodynamics of a chemical reactor is in the focus of this work. The chemical transformations that occur within a reactor are currently ignored. Furthermore, similar to [10], it is assumed that the petroleum feedstock completely evaporates within the nozzles' inlets and enters a riser in a form of gas. This can be partially justified by the fact that a typical time of complete evaporation of a droplet with a diameter of 100 µm in an FCC unit varies from 0.3 to 30.0 ms [15], which is less than the residence time of a feedstock droplet in an injection nozzle, which is above 30 ms for velocities obtained in the current simulations as reported below. Thus, it is assumed that there are only two phases in a riser, the primary (gaseous) phase that represents the mixture of two gases (petroleum feedstock and water vapor) and the secondary (granular) phase that denotes the fluidized zeolite particles dispersed in gas. The feedstock in this study is modeled by gasoil vapor, as the physical properties of this gas are very close to the properties of the feedstock from a real commercial unit.

The modeling is based on a two-fluid Eulerian-Eulerian approach assuming that gas and granular phase are two interpenetrating continua, with no strict boundaries (no interfaces) and no surface tension properties that may be associated with interfaces. Particles of the granular phase are assumed to be very small, i.e., much smaller than any other geometric dimensions, of spherical shape, and all particles are characterized by the same diameter. It is supposed that all collisions are elastic.

To characterize the distribution of the phases in a reactor, we introduce two volume fractions, α_g[1)] and α_s, are introduced which are the relative volumes of the phases in a fluid particle. The range of the granular volume fraction is however limited by the maximum packing density, which is taken as $\alpha_{s,max} = 0.63$.

There is another limiting value for the granular volume fraction (in this work this other limit is taken to be $\alpha_{s,max} = 0.61$), $\alpha_{s,m\ in} = 0.61$), which sets the limit when particles are already in a constant contact with each other and friction forces between the particles are essential. In particular, when $\alpha_s < \alpha_{s,min}$, the granular phase is diluted, particles are far from each other, and collision is the only interaction that occurs between particles. It is further assumed that collisions do not result in formation of agglomerates. For modeling the flow of diluted particle mixtures, one can adopt the kinetic theory of granular flow (KTGF) that represents the granular phase as a gas of very large molecules, and the kinetic properties of the granular phase are then derived from the standard kinetic formulae. In the opposite case of a dense medium, when $\alpha_s > \alpha_{s,min}$, particles of the granular phase are in a constant contact with each other, which renders the KTGF approach invalid. In this case friction forces between particles predefine the kinetic properties of the granular phase.

In the framework of the Eulerian approach, all quantities that define the granular phase are determined by averaging over a small volume (a fluid particle), which is much smaller than the size of a reactor, but, at the same time, which already includes a large number of particles. For instance, the velocity of the granular phase, $\vec{v}_s$, is defined as the mass-averaged velocity of a large number of particles enclosed in a fluid particle, $\vec{v}_s = \vec{u}_s$. Here, $\vec{u}_s$ is the instantaneous (random) velocity of a single particle, and … stands for volume averaging).

Except for the areas in the very vicinity of the nozzle of the pipe that is used for the injection of particles into a reactor, the condition $\alpha_s < \alpha_{s,min}$ is satisfied, and thus the KTFG theory can be employed. Following the classical kinetic theory, the KTFG theory introduces the temperature of the granular phase that is defined as a quantity proportional to the averaged kinetic energy of the random chaotic movements of particles:

$$\frac{3}{2}\theta_s = \frac{1}{2}\langle \vec{u}_s \vec{u}_s \rangle \tag{1}$$

In this work, the movements of zeolite particles with a density of $\rho_s = 2100\,\mathrm{kg\,m^{-3}}$ and a typical diameter of $d_s = 8\times10^{-5}$ m dispersed in a gas mixture are examined. The zeolite particles are lifted up by the gas flow. Nevertheless, the solid particles remain rather heavy, and the transfer of energy from gas to solid particles is negligible. Additionally, just a few collisions between particles can occur due to short residence times of particles in a reactor. The granular temperature, θ_s, is calculated using the approach that neglects the convective and diffusive terms (called the "algebraic" approach in ANSYS Fluent). The granular temperature that is obtained in the calculations always remains very low almost in the entire flow domain (see, e.g., Fig. 6). Low (near zero) values of the granular temperature make other parameters, which characterize the granular phase, also close to zero almost in the entire flow domain.

The above conclusion that all parameters that characterize the granular phase remain rather low is however not applicable for the areas of larger particle concentrations, which are near

1) List of symbols at the end of the paper.

the injection nozzle. In the denser areas, the probability of collisions between particles, $g_{0,ss}$, becomes very high making the values of the granular parameters larger. Furthermore, the viscosity of the granular phase becomes particularly large in the areas where $\alpha_s > \alpha_{s,min}$, when friction between particles dominates the dissipation in the fluid flow.

Another important mechanism for the dissipative losses is provided by turbulence. The dynamics of intensive turbulent flows is modeled. The governing equations are averaged over small time and spatial scales that characterize the turbulent fluctuations. The effects of the turbulent fluctuations enter the averaged equations through the empirical turbulent viscosity and diffusivity coefficients. The coefficients of turbulent viscosity turn out to be significantly stronger than the molecular viscosity of the gas phase and the granular viscosity of the solids phase, again with an exception of the area near the catalyst inlet, where the granular friction viscosity coefficient is particularly large. Likewise, the turbulent diffusivity overwhelms the molecular diffusivity.

3 Geometry and Numerical Mesh

For numerical computations the 3D geometry is built according to the dimensions of the S-200, KT-1/1 catalytic cracking riser, which are summarized in Tab. 1.

Table 1. Dimensions of S-200, KT-1/1 riser.

Parameter	Value
Riser length	40.3 m
Riser diameter	1.3 m (with rising up to 1.4 m)
Nozzle diameter	0.16 m
Nozzle length	0.3 m
Number of nozzles	4
Feedstock input angle	30°
Diameter of the catalyst inlet pipe	1.3 m

In this work, the primary goal is to model the processes that occur in a central part of a riser. The representation of secondary parts is simplified, which are used for the injection of feedstock and regenerated catalyst. Namely, the feedstock is fed into the reactor through several nozzles that are symmetrically distributed at the bottom of the lift reactor (see Fig. 1). As mentioned earlier, the feedstock is injected in the form of small dispersed droplets, although, it is assumes that within the injection nozzles these droplets are fully evaporated. In this work, the conversion of feedstock from liquid to gas state is not modeled, which makes the detailed reproduction of a real geometry of the injection nozzles unnecessary. Thus, the length of the nozzles is reduced from 1.523 m to 0.3 m, and it is simply assumed that the feedstock is fed in the form of gas. Additionally, the feedstock is usually mixed with water vapor injected in the form of droplets dispersed in water vapor. In the current simulations, this representation is also simplified by assuming that only pure feedstock is injected.

Figure 1. Geometry of an FCC riser.

At the very bottom of the lift reactor there is an inclined pipe that is used for the injection of particles of regenerated catalyst. In the model, the length of this pipe is reduced twice, to 6.3 m. It is assumed that the details of the movement of the catalyst particles through the injection pipe are irrelevant for the performance of the lift reactor. It is much more important to understand the speeds and distribution of particles in the main reactor which is studied. The catalyst particles are lifted up into the reactor by the flow of water vapor which is fed through the opening at the very bottom. The gases and catalyst particles leave the reactor through the top end.

The governing equations are summarized in Sect. S1 of the Supporting Information. The equations are supplemented with the boundary conditions. In particular, the standard wall functions are imposed for the velocities. For the gas species also the condition of no-penetration (zero diffusive flux) at the walls is set. The conditions at the inlets are discussed in the following sections. The pressure-outlet condition is imposed at the reactor's outlet. The further details of the numerical solution are reported in Sect. S2 of the Supporting Information.

4 Numerical Results

4.1 Validation

For verification of the model, first the numerical results are compared against the data reported by Young et al. [10]. There are a few important differences between our model and the model in [10]. Firstly, the results reported in [10] are obtained for the full physicochemical model that takes into account the chemical transformations, adopting the eleven-lump kinetic model and reporting that modeling of 30 s of a process requires about three months of calculations. Secondly, the dimensions of the reactors are different, in particular, the diameter of the reactor is 2.5 m in [10]. Thirdly, in [10], significant attention is given to the uniformity of the velocity profile of catalyst particles across a riser. The regenerated catalyst is fed into a riser asymmetrically through the pipe that is attached at one side of a riser, and hence some non-uniformity should be expected.

Nevertheless, in [10], the authors observed that above the feedstock injection the velocity profiles are quite uniform, slightly with higher velocities of catalyst particles near walls as compared with the velocities in the middle of a riser. One of the goals of [10] was to investigate whether additional nozzles could make the profile of catalyst velocity even more uniform. In particular, in [10], the geometry includes the nozzles for slops at the top of a riser to maintain pressure and the group of the nozzles to control temperature. These additional elements are not included in the current work.

Nevertheless, there are some important similarities between the physical models, including the two-fluid modeling approach, and between the geometries, which substantiate this choice for verification. To make the results more similar, for the inlet-outlet parameters, the same values are adopted as reported in [10], which are also summarized in Tab. 2.

The primary interest is the mixing of gases and catalyst particles in a riser. In Figs. 2 and 3 the fields of velocities and volume fractions for each phase are depicted. In these figures, first, it is interesting to analyze the motion and distribution of catalyst particles. One sees that the velocity of catalyst particles rises along the length of the reactor, reaching values of up to 50 m s^{-1} near the feedstock nozzles; see Fig. 2. Below the feedstock injection, catalyst particles are brought into motion by the flow of water vapor. Above the feedstock injection, particles are further accelerated by the fast flow of the feedstock. The volume fractions of catalyst in the bottom section of a riser are relatively high and could reach volume fractions close to 55 %. At the upper parts of a riser, above the feedstock injection, the volume fractions of catalyst decrease to about 20 %. The distribution of catalyst particles is non-uniform in the side injection pipe, but the distribution of particles becomes quite uniform in the main section of a lift reactor.

By comparing the results with the profiles shown in [10], it is found that the velocity profiles, both magnitudes and distributions of velocities, look very similar. Likewise, the distributions of catalytic particles in a reactor agree with [10], demonstrating a similar retention of particles under the feedstock nozzles. Thus, it can be concluded that the hydrodynamic model that we developed is able to capture the main hydrodynamic features of the gas-solid flow in a reactor, producing reasonable flow fields.

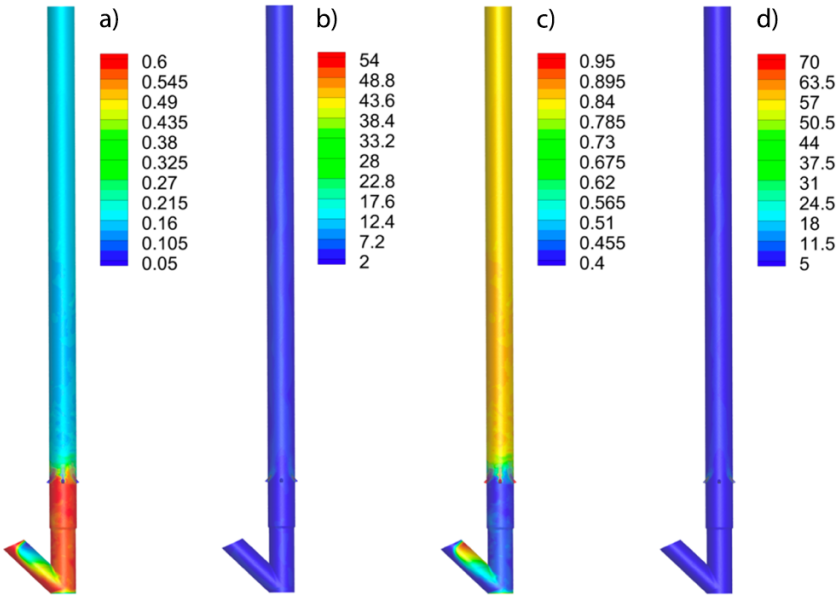

Figure 2. Volume fractions (A, C) and velocities (B, D, in m s^{-1}) of the granular and gaseous phases.

Table 2. Inlet boundary conditions for Yang et al. [10] and S-200, KT-1/1 industrial unit.

Parameter	Value from Yang et al. [10]	Value for S-200m KT-1/1
Feedstock mass flow rate for four nozzles [kg s^{-1}]	–	63.30
Feedstock injection velocity [m s^{-1}]	55.6	–
Water-vapor mass flow rate [kg s^{-1}]	0.82	0.83
Catalyst mass flow rate [kg s^{-1}]	1740	533.47
Catalyst volume fraction	0.6	0.6

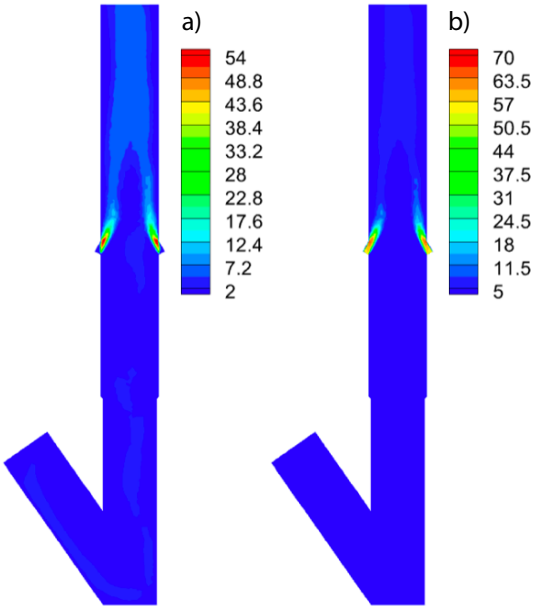

Figure 3. Velocity profiles of the granular (A) and gaseous (B) phases near the feedstock injection nozzles. Velocities are in $m\,s^{-1}$.

4.2 Hydrodynamic Modeling of S-200 KT-1/1 Catalytic Cracking Unit

Next, the operating and boundary conditions are changed by adopting the parameters of the S-200, KT-1/1 industrial unit that is installed in one of the Kazakhstan's refineries. These parameters are also summarized in Tab. 2.

The input parameters for the S-200, KT-1/1 industrial unit differ from the parameters of [10]. The catalyst particles are injected with lower mass rates. The major difference seems to be the higher flow rates of the feedstock injection. For the new input parameters, feedstock velocities at the ends of the injection nozzles are higher, reaching $95\,m\,s^{-1}$. The velocity of the granular phase at this location reaches values of 50–70 $m\,s^{-1}$. As a result, it is observed that in the upper part of a riser, above the feedstock injection, the volume fractions of the catalyst phase are particularly low, reaching only 0.16. Below the feedstock injection one can also observe that the water vapor velocity is about the same level as in [10]. In addition, owing to the lower injection rates of the granular phase and due to the faster flows in the main reactor, the volume fractions of the catalyst particles before the feedstock injection zone remain rather low reaching only 0.44 (Fig. 4).

Fig. 5 depicts the fields of the granular temperature and turbulent kinetic energy. This figure is presented to support our earlier statements that the granular temperature remains low in the entire flow domain. On the contrary, the turbulent kinetic energy is particularly high, especially near the feedstock injection nozzles. The turbulent dissipation and turbulent diffusion are the key effects to define the distributions of the catalyst particles in the reactor.

Finally, in Figs. 6 and 7 the radial profiles of the velocity and volume fractions of the granular phase are displayed. The four different sections of the lift reactor, below the feedstock injection, just above the injection, and at some distances from the injection are depicted. One can notice that the distribution of particles below the feedstock injection is slightly non-symmetrical due to non-symmetrical injection of particles. Just above the feedstock injection the four strong jets are seen that enter the reactor. These jets make the fields of velocity and volume fraction highly non-uniform. However, at the height of 5 m from the feedstock injection, the distribution of particles change again. The distribution becomes very homogeneous, seemingly due to strong turbulent diffusion. The distribution of particles remains homogeneous at all other heights.

5 Conclusion

The hydrodynamics of an FCC riser is studied by adopting the two-fluid approach for a detailed 3D modeling of complex turbulent flows of a gas-solid mixture. The aim was to identify the most important effects that define the hydrodynamics of the reactor, and to obtain an efficient numerical model for 3D modeling of the physicochemical processes in the reactor. In particular, it was found that in the main part of the lift reactor the granular mixture is sufficiently diluted, so the KTFG model can be applied for calculation of the physical properties of the granular phase. Although, it was stated that the values of the granular temperature, pressure, and other parameters of the granular phase are very low, except for the zones near the injection of catalyst particles.

The inclusion of molecular and granular viscosities as well as the molecular diffusivity turned out to be completely unnecessary, as these effects are highly overpowered by the turbulent

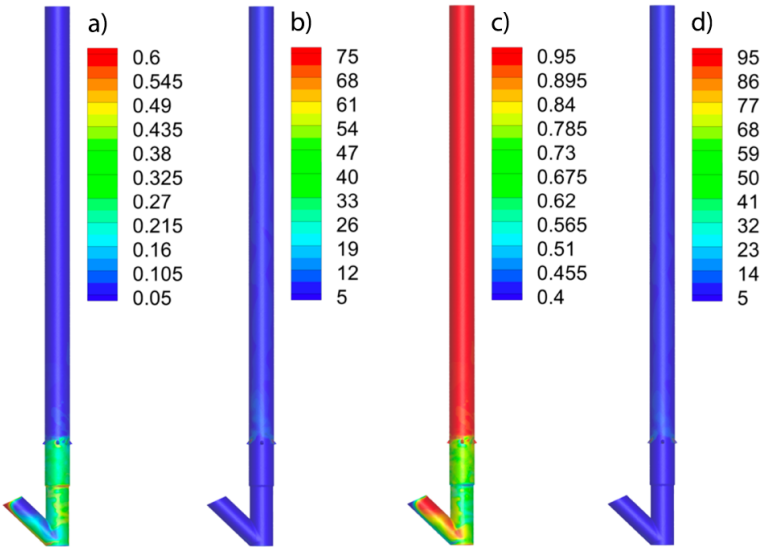

Figure 4. Profiles of volume fractions (A, C) and velocities (B, D, in $m\,s^{-1}$) of the granular (A, B) and gas (C, D) phases in a riser of the S-200 KT-1/1 unit.

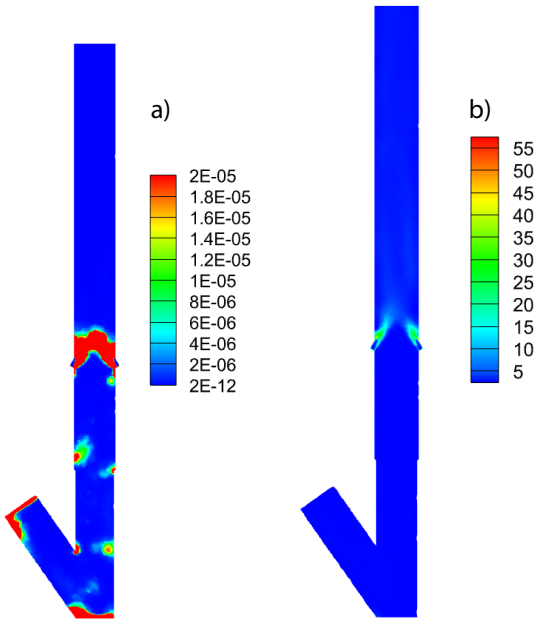

Figure 5. Granular temperature (A) and kinetic energy of turbulent fluctuations (B). Both quantities are in J kg^{-1}.

viscosities and diffusivities. The major effect that explains the lifting up of catalyst particles is the momentum exchange between the phases that is based on the drag forces calculated for solid particles. The distribution of particles in the reactor is dominated by the geometry of the reactor and by the turbulent diffusion.

The turbulent diffusion explains the nearly homogeneous distributions of the catalyst particles in the main length of the riser, which is highly desirable for an efficient operation of the FCC reactor. The reaction times are determined by the speed of the gas-solid mixture, which is controlled by the injection flow rates of the feedstock and water vapor.

The model is applied for the analysis of the mixing dynamics of gases and particles in a riser from the S-200 KT-1/1 unit, predicting the distributions of velocities of catalyst and hydrocarbons. The model and the numerical results will serve as a guideline for the revision and optimization of the industrial unit. In future, it is intended to improve the model by adding the reactions of catalytic cracking to predict distribution of cracking products and thus to predict the overall yields of this technological process.

Supporting Information

Supporting Information for this article can be found under DOI: https://doi.org/10.1002/ceat.202100596. This section includes additional references to primary literature relevant for this research [16–18].

Acknowledgment

The reported study was funded by the Russian Foundation for Basic Research (grant No. 21-53-10004) and by the Royal Society (grant IEC\R2\202051).

The authors have declared no conflict of interest.

Symbols used

C_d	[–]	drag coefficient
d_s	[m]	diameter of solid particles
D_g	[kg m^{-2}s^{-1}]	gas molecular diffusivity
e_{ss}	[–]	coefficient of restitution of particle collisions
g	[m s^{-2}]	gravity acceleration

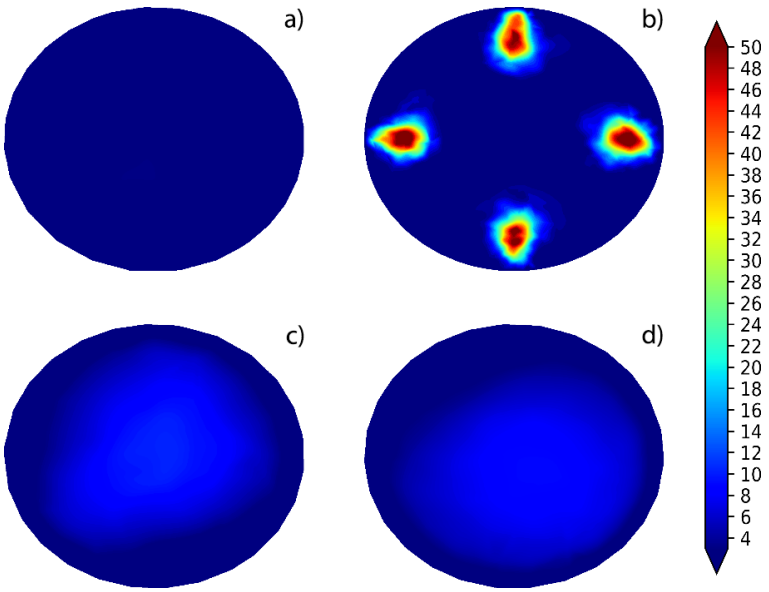

Figure 6. Radial profile of the granular phase velocity (in m s^{-1}) at 5 m (A), 6.5 m (B), 10 m (C), and 15 m (D) from the reactor's bottom.

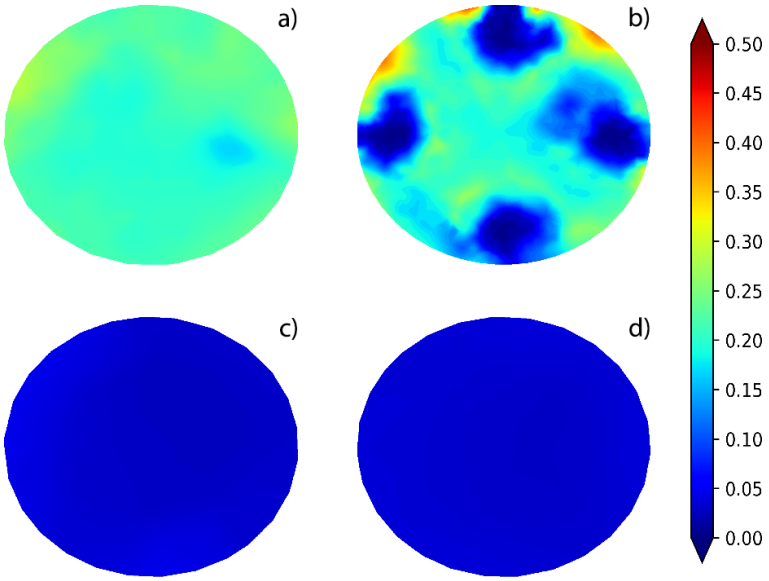

Figure 7. Radial profile of granular phase volume fraction at 5 m (A), 6.5 m (B), 10 m (C), and 15 m (D) from the reactor's bottom.

$g_{0,ss}$	[–]	probability of collisions between particles
I	[–]	unit tensor
I_{2D}	[s^{-2}]	second invariant of the deviatoric stress tensor
k	[$J\,kg^{-1}$]	turbulent kinetic energy
k_s	[$kg\,m^{-1}s^{-1}$]	diffusion coefficient
p	[Pa]	pressure
Re	[–]	Reynolds number
Sc_t	[–]	turbulent Schmidt number
t	[s]	time
v	[$m\,s^{-1}$]	velocity
Y	[–]	mass fraction

Greek letters

α	[–]	volume fraction
$\alpha_{s,max}$	[–]	maximum packing density
$\alpha_{s,min}$	[–]	upper limit for the KTFG approach
β	[$kg\,m^{-3}s^{-1}$]	fluid-solid exchange coefficient
γ_s	[$J\,m^{-3}s^{-1}$]	collisional rate of energy dissipation per unit volume
ε	[$J\,kg^{-1}s^{-1}$]	dissipation rate of turbulent fluctuations
θ_s	[$J\,kg^{-1}$]	granular temperature
λ	[$kg\,m^{-1}s^{-1}$]	bulk viscosity
μ	[$kg\,m^{-1}s^{-1}$]	shear viscosity
ρ	[$kg\,m^{-3}$]	density
τ	[$kg\,m^{-1}s^{-2}$]	viscous stress tensor
φ	[–]	angle of internal friction
φ_{gs}	[$J\,m^{-3}s^{-1}$]	rate of transfer of kinetic energy between particulate and gaseous phases

Sub- and superscripts

1,2	petroleum feedstock (1) and water vapor (2)
g	gas
m	mixture
s	solid
t	turbulent
T	transpose

Abbreviations

FCC	fluid catalytic cracking
KTGF	kinetic theory of granular flow

References

[1] B. Amblard, R. Singh, E. Gbordzoe, L. Raynal, *Chem. Eng. Sci.* **2016**, *170*, 731–742. DOI: https://doi.org/10.1016/j.ces.2016.12.055

[2] V. W. Weekman Jr., D. M. Nace, *AIChE J.* **1970**, *16*, 397–404. DOI: https://doi.org/10.1002/aic.690160316

[3] S. M. Jacob, B. Gross, V. M. Weekman, *AIChE J.* **1976**, *22 (4)*, 701–703. DOI: https://doi.org/10.1002/aic.690220412

[4] G. Nazarova, E. Ivashkina, E. Ivanchina, A. Oreshina, E. Vymyatnin, *Fuel Process. Technol.* **2021**, *217*, 106720. DOI: https://doi.org/10.1016/j.fuproc.2020.106720

[5] G. Y. Nazarova, E. N. Ivashkina, E. D. Ivanchina, A. V. Vosmerikov, L. N. Vosmerikova, A. V. Antonov, *Catalysts* **2021**, *11 (6)*, 701. DOI: https://doi.org/10.3390/catal11060701

[6] G. Nazarova, E. Ivashkina, T. Shafran, A. Oreshina, G. Seitenova, *Pet. Sci. Technol.* **2020**, *38*, 1017–1025. DOI: https://doi.org/10.1080/10916466.2020.1825966

[7] G. Nazarova, E. Ivashkina, E. Ivanchina, A. Oreshina, E. Vymyatnin, G. Burumbaeva, *Pet. Sci. Technol.* **2020**, *38 (12)*, 754–762. DOI: https://doi.org/10.1080/10916466.2020.1779290

[8] G. Y. Nazarova, V. A. Chuzlov, E. D. Ivanchina, E. N. Ivashkina, U. N. Kopycheva, I. O. Dolganova, *Pet. Coal* **2020**, *62 (4)*, 1250–1255.

[9] J. Gan, H. Zhao, A. S. Berrouk, C. Yang, H. Shan, *Ind. Eng. Chem. Res.* **2011**, *50*, 11511–11520. DOI: https://doi.org/10.1021/ie100232h
[10] Q. Yang, A. S. Berrouk, Y. Du, H. Zhao, C. Yang, M. A. Rakib, A. Mohamed, A. Taher, *Appl. Math. Model.* **2016**, *40*, 9378–9397. DOI: https://doi.org/10.1016/j.apm.2016.06.016
[11] G. C. Lopes, L. M. Rosa, M. Mori, J. R. Nunhez, W. P. Martignioni, *Int. J. Chem. Eng.* **2012**, *2012*, 1–16. DOI: https://doi.org/10.1155/2012/193639
[12] S. Chen, Y. Fan, Z. Yan, W. Wang, X. Liu, C. Lu, *Chem. Eng. Sci.* **2016**, *153*, 57–74. DOI: https://doi.org/10.1016/j.ces.2016.07.003
[13] W. Huang, A. Yan, J. Zhu, *Chem. Eng. Technol.* **2007**, *30 (4)*, 460–466. DOI: https://doi.org/10.1002/ceat.200600400
[14] M. N. Idris, A. Burn, *AIChE 2008 Annual International Conference*, November 16-21, **2008**.
[15] A. C. Barbosa, G. C. Lopes, L. M. Rosa, M. Mori, W. P. Martignoni, *AIDIC Conf. Ser.* **2013**, *11*, 31–40. DOI: https://doi.org/10.3303/ACOS1311004
[16] ANSYS Fluent Theory Guide, Release 2021, January **2021**, ANSYS Inc.
[17] D. G. Schaeffer, *J. Differ. Equations* **1987**, *66*, 19–50. DOI: https://doi.org/10.1016/0022-0396(87)90038-6
[18] D. Gidaspow, R. Bezburuah, J. Ding, in *Proc. of the 7th Engineering Foundation Conf. on Fluidization*, Engineering Foundation, New York **1992**, 75–82.

